Article

Not peer-reviewed version

CH4 Adsorption in Wet Metal-Organic Frameworks Under Gas Hydrate Formation Conditions Using Large Reactor

Jyoti Shanker Pandey * , Nehir Öncü , Nicolas Von Solms

Posted Date: 16 April 2024

doi: 10.20944/preprints202404.1006.v1

Keywords: Metal Organic Framework; high pressure isotherms; gas hydrates; CH4 storage

 doi:10.20944/preprints202404.1006.v1

Article

CH_4 Adsorption in Wet Metal-Organic Frameworks Under Gas Hydrate Formation Conditions Using Large Reactor

Jyoti Shanker Pandey [1,2]*, Nehir Öncü [1,3], Nicolas von Solms [1]

[1] Center for Energy Resource Engineering (CERE), Department of Chemical Engineering, Technical University of Denmark, 2800 Kgs. Lyngby, Denmark
[2] Laboratorio de Materiales Avanzados, Departamento de Qu´ımica Inorg´anica-Instituto Universitario de Materiales, Universidad de Alicante, Ctra. San Vicente-Alicante s/n, E-03690 San Vicente del Raspeig, Spain
[3] Department of Chemical Engineering, Middle East Technical University, 06800 Ankara, Türkiye
* Correspondence: jyshp@kt.dtu.dk

Abstract: Nanoporous materials, such as Metal-Organic Frameworks (MOFs), are renowned for their high selectivity as gas adsorbents due to their specific surface area, nanoporosity, and active surface chemistry. A significant challenge for their widespread application is their behavior and reduced gas uptake in wet conditions, attributed to competitive adsorption between gas and water. The current understanding of gas adsorption in wet materials is constrained by studies that utilize only small amounts of powdered porous materials (in the milligram range) within very small reactors (1-5 mL). This leaves a significant gap in knowledge about gas adsorption behaviors in larger reactors and when MOF sample sizes are increased (to the gram scale) for scaling up the process. Additionally, there is a notable dearth of experimental research in situations where MOFs are heavily saturated with water. To address these gaps, this study measures CH_4 adsorption in MOFs under conditions of high moisture content, using larger samples of MOFs (in grams) and a large volume reactor. We selected commercially available MOFs, including HKUST-1, ZIF-8, MOF-303, and activated carbon. A high-pressure isotherms (at T = 274.15 K) using volumetric approach were measured to qualitatively compare the moles of gas adsorbed under both dry and wet conditions across different MOFs and weights. Experimental results show that the presence of water led to a decrease in total CH_4 mmol adsorption in MOFs, with a more significant decrease observed in hydrophilic MOFs compared to hydrophobic ones. For hydrophilic MOFs, presence of crossover isotherms at crossover pressure provided evidence of water's conversion to hydrate and its positive role in enhancing total gas uptake, which varied among different hydrophilic MOFs. Oversaturated MOFs showed a larger deviation between dry and wet cases at higher pressures. The high-pressure isotherm data confirm the positive role of hydrophilic MOFs in the conversion of water to hydrate in oversaturated MOFs when MOFs sample size is large.

Keywords: metal organic framework; high pressure isotherms; gas hydrates; CH_4 storage

1. Introduction

Gas hydrates represent an intermediate phase between ice and water, formed under high pressure and low temperature conditions. They are formed when water molecules create a cage-like structure through hydrogen bonding, with stability provided by guest molecules such as gaseous CH_4 (methane) and CO_2 (carbon dioxide). The thermodynamics, kinetics, and stability of gas hydrates are influenced by differences in guest molecules and the properties of water [1]. The formation of gas hydrates is a stochastic phenomenon, characterized by low water-to-hydrate conversion rates and slow formation kinetics. As a result, various improvements have been proposed, including the use of chemical promoters, mechanical stirring, or the employment of porous materials to enhance the contact area between gas and liquid. Recent advances suggest the potential of hydrate formation in

 doi:10.20944/preprints202404.1006.v1

nanospaces as well as on the outer surfaces of nanoporous materials [2–4]. Examples of such nanoporous materials include metal-organic frameworks (MOFs), zeolitic imidazolate frameworks (ZIFs), and activated carbon, among others

Methane (CH_4) gas has a significantly lower volumetric energy density (0.0107 MJ/L) compared to traditional petroleum fuels, such as gasoline (34.2 MJ/L), which reduces its viability for commercial-scale applications [5]. The volumetric energy density can be enhanced through compression or liquefaction processes [6]. Adsorption is viewed as a promising technology for high-density gas storage of CH_4 under mild conditions, requiring only a single compression step [7]. Traditionally, adsorption-based technologies have relied on zeolite and carbon materials due to their straightforward synthesis process on a commercial scale. Nanoporous materials, such as Metal-Organic Frameworks (MOFs), are recognized as effective gas adsorbents through physisorption, typically under high temperature and moderate pressure. Key factors influencing this process include the MOFs' surface area, surface chemistry (including hydrophobic or hydrophilic characteristics), and pore size. The development of Metal-Organic Frameworks (MOFs) with potentially enhanced adsorption capacities and lower energy requirements for regeneration has attracted attention from the scientific community. MOF development allows for the precise control of pore size, geometry, and functionality [8]. HKUST-1 is among the most studied MOFs for CO_2 and CH_4 adsorption, as its open metal sites exhibit robust interactions with gas molecules [9].

A significant challenge in physisorption is the presence of water vapor or humidity in the incoming gas stream, which competes with the gas for adsorption sites on the MOFs' surface, thereby reducing the total gas adsorption capacity. Prolonged exposure to water vapor can also lead to MOFs degradation, resulting in their structural instability [10]. Gas hydrate crystals could thus be useful in addressing this issue, as introducing a phase change in the presence of nanoporous materials could convert water into hydrates. By inducing a phase change with nanoporous materials, we could: (1) convert water into hydrate crystals, thereby prolonging the chemical stability of MOFs, and (2) save energy through low-temperature-based hydrate formation. Based on these hypotheses, researchers have explored various types of nanoporous materials to investigate the hydrate formation phenomenon for pure gases like CH_4[3,11], CO_2, and H_2[12].

Most studies on MOFs' application in improving gas hydrate technology focus on CH_4 hydrate formation. Available studies show that many MOFs including MIL-53 [13,14], MIL-100 [15], ZIF-8 [14,15], HKUST-1 [3,14], Cr-based MOF-1, and Y-shaped MOF-5 [4] are covered in recent studies. ZIF-8 and HKUST-1 are most extensively studied MOFs in gas hydrate research. HKUST-1 is a hydrophilic MOFs while ZIF-8 is a hydrophobic MOF. ZIF-8 and HKUST-1 are also different in terms of thermal conductivity (HKUST-1 = 0.44–0.73 W/(m K) [16], ZIF-8 = 0.32 W/(m K) [17]). Higher thermal conductivity supports faster heat dissipation during hydrate formation.

In the case of MIL-53, CH_4 hydrates form in meso- and macroporous spaces and interparticle spaces, with no hydrate formation in micropores [13]. Recent studies indicate that hydrophilic MOFs like MIL-100 (Fe) impede hydrate formation when exposed to moisture, leading to a decrease in gas density at the water-MOF interface. Conversely, hydrophobic MOFs such as ZIF-8 facilitate gas hydrate formation [15]. Experimental data suggests that hydrophilic surfaces obstruct gas hydrate nucleation due to disrupted water structures within the pores. In contrast, on hydrophobic surfaces, dissolved gas molecules accumulate, forming surface nanobubbles due to hydrophobic attraction.

Current experimental studies on gas adsorption in wet nanoporous materials involve two different approaches. In the first approach, High pressure differential calorimetry is used to study the water to hydrate conversion under high pressure (80-100 bars). For example in recent studies using HKUST-1[3] and ZIF-8 [11], authors showed that hydrates predominately formed at the outer surface of the MOFs and water/solid ratio controlled the spread of water over the surface. In another set of studies, high pressure volumetric isotherm based method was used to measure gas adsorption (in mmol/gram) in wet nanoporous materials to compare and calculate positive contribution of hydrate formation in total gas mole adsorption under different water saturations but at constant material weight [4,15].

 doi:10.20944/preprints202404.1006.v1

The conclusions from recent studies are limited by small sample sizes. Additionally, there is a notable dearth of experimental research in situations where MOFs are heavily saturated with water. To address these gaps, we investigate the competitive adsorption of CH_4 gas and water in nanoporous materials under hydrate formation conditions (T = 274.15 K and upto 80 bars) using a large-volume reactor and larger sample sizes to better understand the behavior for process scaling. Furthermore, we explore how the degree of wetness affects gas adsorption and the role of material properties in influencing adsorption behavior.

2. Materials and Methods

2.1. Setup and Materials

All nanoporous materials used in this study are procured commercially and their basic characteristics are provided in Table 1. ZIF-8 (Basolite® Z1200), HKUST-1 (Basolite® C 300) were procured from Sigma-Aldrich. MOF-303 (3,5-Pyrazoledicarboxylic acid monohydrate) was procured from novoMOF, Activated carbon (AC) was procured from NuChar. Before the experiments, the MOFs were heated up to 120°C in a vacuum oven for 24 hours to get rid of any impurities. The Ultrapure water used to wet the MOFs during the experiments was created inside the lab using setup from Merck Millipore. ZIF-8 and NuChar AC are characterized as hydrophobic materials while HKUST-1 and MOF 303 are characterized as hydrophilic materials.

HKUST-1 ($Cu_3(BTC)_2$) is comprised of copper nodes linked by 1,3,5- benzenetricarboxylic acid and bimodal pores [18]. Some of the key advantages of HKUST-1 for CH_4 adsorption is its large internal pore diameter, high thermal conductivity and supportive surface chemistry that could lead to high methane uptake [19,20] and water adsorption [21] such that water to gas contact area increases on account of higher wettability. High thermal conductivity of HKUST-1 could be on account of copper at metal nodes that could help remove local heat of hydrate formation.

Table 1. Commercial available data information of MOF/nanoporous materials.

Sample Type	HKUST-1	ZIF-8	MOF 303	NuChar Carbon
BET Surface area (m^2/g)	641	1550	1133	1366
Adsorption energy (kJ/mol)	35.51		32.29	16.54
Density	0.88	0.95	0.40	0.40
Procurement	Sigma Aldrich	Sigma Aldrich	NovoMOF	Nuchar
Purity	99%	99%	99%	99%

The high-pressure adsorption and desorption experiments on solid materials (both dry and wet) were conducted using the apparatus depicted in Figure 1. This system comprises a high-pressure reactor, a cylinder with piston, and a Vindum pump. The reactor, which has a total volume of 210 cm^3 and a maximum design working pressure of 150 bar, is connected to a bath system for temperature control. It is utilized for placing dry and wet solid materials for gas adsorption and desorption studies. Additionally, there is a cylinder with a movable piston; the gas portion is connected to the reactor, and the water portion is linked to the Vindum pump.

 doi:10.20944/preprints202404.1006.v1

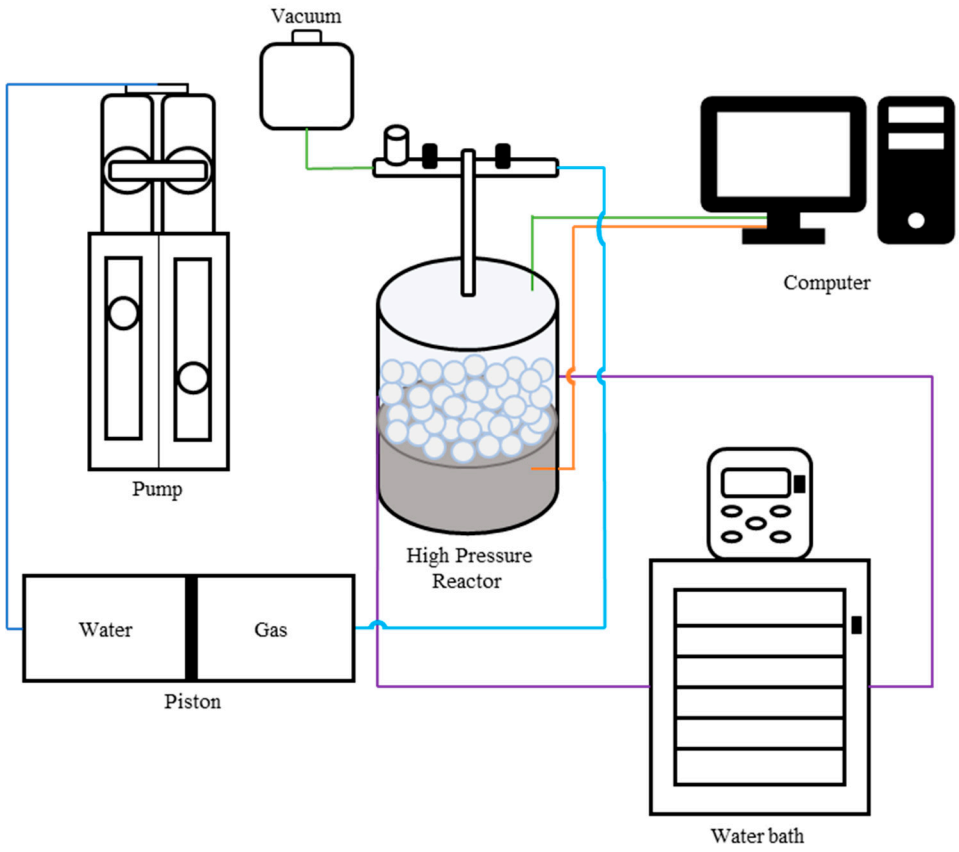

Figure 1. Systematic diagram of the experimental apparatus.

The Vindum pump are used to use water pressure to regulates the reactor's pressure and facilitates adsorption and desorption experiments via stepwise pressurization and depressurization. A thermometer is installed at the reactor's bottom to measure the in-situ temperature. The uncertainties in temperature and pressure measurements are ±0.1 K and ±0.5 bar, respectively. Changes in the system's pressure, temperature, and volume are continuously recorded. In the reactor, glass beds and glass cottons are placed after the material to reduce the dead volume. Studies were performed for both samples and blank reactor to measure and eleimiate the contribution of the dead volume.

2.2. Procedure and Data Processing

2.2.1. Gas Adsorption & Desorption Experiment

Dry material with a known weight (in grams) is placed in a reactor with a known volume, followed by a metal mesh. The remaining volume above the metal mesh is filled with glass beads and glass cotton to minimize the dead volume. The metal mesh is placed to prevent the glass beads from mixing with the materials. The reactor is then sealed, and leak testing is performed. Before the CH_4 gas adsorption experiment, a vacuum is applied to remove any air pockets. In the first stage of gas injection, methane gas is introduced into the reactor until the pressure reaches 20 bar, which is then maintained for two hours. Initially piston is filled with gas at 20 bar and later connected with reactor. Piston movement is balanced through water pump such that reactor reached to 20 bar while water side of piston is in equilibrium with gas side at 20 bar. Total water volume was measured which was equal to amount of gas injected into reactor contaiing material. Thereafter, pressure inside the reactor is increased in a stepwise manner using water pump, starting with 20 bar followed by increments of 5 bar. At every step, the pressure is kept constant for 2 hours to ensure the system reaches equilibrium. Total water volume injected into piston is calculated and adjusted with piston volume to calculate total volume of gas being used. The experiment is concluded when the system achieves

 doi:10.20944/preprints202404.1006.v1

equilibrium at 80 bars. The total duration of each experiment is approximately 42 hours. During this time, the change in the total volume of gas on the MOF side is measured to calculate the total moles of gas being adsorbed.

For each material, the experiment is conducted for the dry case followed by the wet cases. At the end of the dry case, water with known quantity is added to introduce such that water/solid ratio (gram/gram) (Rw) is progressively increased from 0.5, 1, 1.5, 2..and so on. Thus, the same material with same weight is being used until the full completion of all of its experiments. Weight of the material was varied between different materials due to commercial availability thus, Rw was adjusted as per the weight of the material used in the experiment and therefore moles of gases adsorbed are reported for per gram for accurate comparison across different experiments and materials.

Reactor is kept at isothermal conditions (at 274.15K) using water bath. Due to long duration and change in room temperature, temperature variations equals ±0.25°C during the experiment. Gas desorption experiment was performed in selected experiments at the end of adsorption experiments. Once the reactor is pressurized up to 80 bar, given experiment undergoes a gradual depressurization using the stepwise methods with key depressurization steps and rates.

2.2.2. Data Processing Calculations Gas

The customized high-pressure reactor was utilized to measure the total volume of CH_4 gas adsorbed, with the reactor being filled with various MOFs and subjected to different water-to-solid ratios. The temperature within the reactor was maintained at 274.15 K which falls within the hydrate formation zone, to ensure a high driving force for adsorption. Taking into account the known weights and densities of the materials used, including the weights of the glass beads, the empty space inside the reactor—including the voids within the MOFs—was measured. Reactor was connected with gas piston. Gas piston is controlled by the water pump. Pressure inside gas piston is covered through water pump. Total gas volume available in combined piston and reactor is calculated at any given pressure using Equation 1.

$$V_{gas} = V_{piston} - V_{water} + V_{chamber}$$

Where V_{piston} is the total volume of the piston (equal to 1200 cm^3 in this experiment), V_{water} is the volume in the piston occupied by water, $V_{chamber}$ is the volume inside the high pressure reactor occupied by gas, and V_{gas} is the total volume available for CH_4 gas across the piston and reactor, all corresponding to specific pressure value and R_w value. The volume occupied by the moving part inside the piston and the line connecting the piston and the chamber are neglected. Then, to accurately calculate the amount of CH_4 available in the gas piston at the start of the experiment at 20 bar with known volume is converted to number of moles using Equation 2:

$$n_{CH_4,total} = \frac{PV_{piston}}{ZRT}$$

Where $n_{CH_4,total}$ is the total number of CH_4 available in the overall system, P is a specific pressure value, T is the temperature measured simultaneously as the pressure and volume values, Z is the compressibility factor of CH_4 calculated at this temperature, and R is the universal gas constant.

The number of moles of CH_4 available in the system will always be the same if it is ensured that there is no leaking. Consequently, the amount of CH_4 inside the chamber is calculated with Equation 3:

$$n_{CH_4,reactor} = n_{CH_4,total} * (\frac{V_{chamber,MOF}}{V_{gas}})$$

Where $n_{CH_4,reactor}$ is the amount of CH_4 inside the chamber corresponding to any specific pressure value. The n_{CH_4} value includes the CH_4 inside the pores of the MOFs as well as the dead volume. V_{gas} value is achieved when it is assumed that gas and piston reach the equilibrium with in piston and pressure driven adsorption is completed. Higher adsorption, higher drop in V_{gas}.. Typically V_{gas} is sensitive to volume change on account of gas adsorbed and change in the dead volume thus Vgas

 doi:10.20944/preprints202404.1006.v1

would be dependent on adsorptive behavior of different materials as well as different dead volume on account of different mass and Rw values.

To normalized moles of CH4 in MOFs filled reactor, the $n_{CH_4,reactor}$ value is divided by the sample weight (in grams) by using Equation

$$n_{CH_4,MOF} = \frac{n_{CH_4,reactor}}{m_{MOF}}$$

Where $n_{CH_4,MOF}$ is the moles of CH_4 inside the MOFs filled reactor and m_{MOF} is the weight of the MOF sample available inside the reactor. Finally, an isotherm is created ranging from 0 bar to 80 bar for all Rw cases of MOFs to qualitatively understand the comparison. The isotherm is plotted with pressure values on the x-axis and corresponding $n_{CH_4,MOF}$ values on the y-axis.

3. Results

Stepwise pressure build up methodology was used to create high pressure isotherm to analysis water/MOF interactions under isothermal conditions.

3.1. Reproducibility of the Experiment

Selected experiment was repeated to ensure the reproducibility of our results using the method proposed here for varying sample amounts. Table 2 presents the mmol/gram of CH_4 adsorbed on dry ZIF-8 in two distinct experiments with different initial weights. The results confirm the reproducibility of our findings using the described method. Consequently, the same method was utilized to compare gas adsorption values across various materials with different degree of wetness.

Table 2. CH_4 gas adsorbed on ZIF-8 in two different experiments (** Experiment was terminated at P = 70 bars).

	CH_4 Amount adsorbed	**(Reactor Volume = 210 mL)**
	Exp.1#	Exp.2#
Temp (°C)	274.15K	274.15K
Weight (gram)	15	6.3
Pressure (bars)	(mmol/gram)	(mmol/gram)
0	0.00	0.00
20	24.03	22.92
25	28.72	27.54
30	32.74	31.87
35	36.47	36.01
40	39.91	39.59
45	42.85	43.17
50	45.66	46.35
55	48.49	49.24
60	51.26	52.09
65	53.35	54.98
70	55.53	57.60
75	XX*	59.99
80	XX*	62.28

Samples placed in the reactor were never removed, and water was added to the system without its removal. The absolute value of gas adsorbed per gram was calculated by subtracting the blank value from the measured excess adsorption value. This analysis provides a qualitative assessment of the adsorption efficiency at high pressure. The results of this study are dependent on the analytical technique used. For example, the amount of gas molecules adsorbed was determined based on a

 doi:10.20944/preprints202404.1006.v1

stepwise increase in pressure, assuming that a steady state was achieved after maintaining constant pressure for 2 hours.

3.2. Gas Adsorption for Dry Case

Gas adsorption in dry MOFs is controlled by the pore size, surface area and kinetic diameter of the gases. Water kinetic diameter is equal to 0.265 nm, H_2 kinetic diameter is 0.289 nm, CO_2 kinetic diameter is 0.33 and CH_4 kinetic diameter is 0.38 nm [22]. These kinetic diameters are much smaller than the pore size of nanoporous materials (0.7 to 1.2 nm). We have selected 4 nanoporous materials and total CH_4 gas adsorbed is measured and mentioned in Table 3.

Table 3. CH_4 gas adsorbed on dry MOF at 274.15K.

	CH_4 Amount adsorbed (mmol/gram) (RW= 0)			
Temp (K)	274.15	274.15	274.15	274.15
Weight (gram)	6.3	42.1	20.5	17.3
Pressure (bar)	ZIF-8	NuChar-AC	HKUST-1	MOF-303
0	0.00	0.00	0.0	0.0
20	22.92	2.15	5.1	7.2
25	27.54	2.58	5.7	8.5
30	31.87	3.16	6.0	9.7
35	36.01	3.66	6.2	10.8
40	39.59	4.13	6.8	11.7
45	43.17	4.60	7.5	12.6
50	46.35	5.08	7.7	13.3
55	49.24	5.52	8.4	14.0
60	52.09	6.01	9.1	14.7
65	54.98	6.49		15.3
70	57.60	6.78		15.9
75	59.99	6.81		16.0
80	62.28	6.81		16.0

In the dry case, we found that CH_4 gas adsorption among MOFs was highest in ZIF-8, whereas, among hydrophilic MOFs, MOF-303 exhibited a higher CH_4 adsorption capacity compared to HKUST-1. Zeolitic imidazolate frameworks (ZIFs), a subgroup of metal–organic frameworks, exhibit a zeolitic structure due to coordination between transition metal ions (inorganic) and imidazolate ligands (organic) such that framework is composed of tetrahedral structural units similar to zeolites [23]. ZIFs are known for high large surface area, high porosity and are chemically and thermally stable. ZIF-8 is most common among different ZIF variants and thus a popular candidate to capture and store CO_2. [24]. ZIF-8 application for CH_4 adsorption is limited [25]. ZIF-8 exhibits a higher CH_4 gas adsorption capacity than other traditional MOFs, which confirms that ZIF-8 has an expandable framework. This framework further expands at low temperatures and high pressures [26]. ZIF-8 shows lower gas uptake at pressures below 25 bar; however, due to its expandable network, the total gas uptake increases.

The higher CH_4 adsorption capacity of ZIF-8, surpassing that of HKUST-1, has also been observed by other researchers. Generally, HKUST-1 is considered to have a higher CH_4 adsorption capacity compared to other MOFs due to its open metal site. However, neither HKUST-1 nor MOF-303 exhibit any expandable structure under the influence of high pressure.Our study also shows that MOF-303 has higher CH_4 adsorption capacity (1.6 times at P = 60 bar) as compared to HKUST-1 which

 doi:10.20944/preprints202404.1006.v1

can be contributed to higher BET surface area availability for MOF-303. Total adsorption amount increases on account of increase in pressure or lowering the temperature. One of the similar studies, CH_4 adsorption value in HKUST-1 was measured for dry case at 303 K and 315 K [27].

3.3. Gas Absorption Behavior for Wet Material

As described in the methodology, water was introduced into the material in controlled quantities without disturbing its placement in the cell. The Rw was gradually increased from 0.5 to 2, and below, we discuss the role of water in gas adsorption behavior. In this study, we used three different MOFs and one activated carbon, all of which were procured from commercial vendors. There are examples utilizing HKUST-1 for gas adsorption at low temperatures in both dry and wet cases. Since most of the MOFs used in this study have a pore size smaller than 1.2 nm, it is believed that hydrate formation would mostly occur on the surface of the MOFs and activated carbon, thus making hydrophobicity, surface area, and surface chemistry significant factors.

There are lack of studies on CH_4 adsorption in wet mater using high pressure isotherms and there are very few studies that confirmed stepped isotherms or crossover isotherms.

3.3.1. CH_4 gas adsorption in wet hydrophobic nanoporous materials

Table 4. CH_4 gas adsorbed on wet hydrophobic MOFs (Different R_w).

	CH_4 Amount adsorbed in wet hydrophobic material (mmol/gram)							
T (K)	**274.15**					**274.15**		
W (gram)	42.2	42.2	42.2	42.2	42.2	6.3	6.3	6.3
Rw=	0	0.5	1	1.5	2	0	0.5	1.0
P (bar)	NuChar AC (mmol/gram)					ZIF-8 (mmol/gram)		
0	0.0	0.0	0.0	0.0	0.0	0.0	0.0	0.0
20	2.1	1.7	1.2	0.7	0.3	22.9	22.5	22.0
25	2.6	2.0	1.5	0.9	0.4	27.5	26.9	26.3
30	3.2	2.5	1.8	1.1	0.4	31.9	31.0	30.4
35	3.7	2.9	2.1	1.3	0.5	36.0	35.3	34.7
40	4.1	3.3	2.4	1.5	0.6	39.6	38.8	38.3
45	4.6	3.7	2.6	1.7	0.7	43.2	42.4	41.9
50	5.1	4.1	2.9	1.9	0.8	46.4	45.4	45.0
55	5.5	4.4	3.2	2.1	0.9	49.2	48.3	48.0
60	6.0	4.8	3.5	2.2	1.0	52.1	51.2	50.9
65	6.5	5.2	3.8	2.4	1.0	55.0	53.8	53.7
70	6.8	5.6	4.0	2.6	1.1	57.6	56.3	56.2
75	6.8	5.7	4.3	2.8	1.2	60.0	58.6	58.6
80	6.8	6.1	4.6	3.0	1.3	62.3	60.8	60.9

To better understand the competitive adsorption properties between CH_4 and H2O molecules and their connection with the properties of microporous materials, we created adsorption isotherms for HKUST-1 and ZIF-8 materials at a temperature of 274.15 K. The pressure was increased in a stepwise manner, significantly above the stability pressure of the bulk case, to ensure that hydrate formation would occur. All microporous compounds have pore diameters larger than that of the water molecule; however, water molecule penetration into ZIF-8 is not successful due to its hydrophobic surface chemistry [28,29]. In contrast, HKUST-1 and MOF 303 are hydrophilic and

 doi:10.20944/preprints202404.1006.v1

should be able to accommodate water into their pores [30,31]. The variance in the amount of water added to the materials could lead to different distributions of water within the pores and on the surface. These water loadings were evaluated both below and above the total water saturation amount. It is expected that the water saturation value for HKUST-1 is 44%, which suggests that the pores are mainly filled with dispersed water [14].

3.3.2. CH_4 gas adsorption in wet hydrophilic nanoporous materials

HKUST-1 and MOF-303 are both known hydrophilic MOFs with different degrees of water uptake. CH_4 adsorption in wet MOFs were calculated under high pressure low temperature region. It is well known that gas adsorption increases at higher pressure and lower temperature.

Table 4. CH4 gas adsorbed on wet hydrophilic MOFs (Different Rw).

	CH_4 Amount adsorbed in wet and hydrophobic material (mmol/gram)					
T (K)		**274.15**			**274.15**	
W (gram)	20.5	20.5	20.5	17.3	17.3	17.3
Rw=	0	0.85	2.36	0	1	1.5
P (bar)	HKUST-1 (mmol/gram)			MOF 303 (mmol/gram)		
0	0.0	0.0	0.0	0.0	0.0	0.0
20	5.1	4.9	3.5	7.2	6.3	5.9
25	5.7	5.5	4.2	8.5	7.6	7.1
30	6.0	6.0	5.3	9.7	8.8	8.3
35	6.2	6.6	7.2	10.8	10.2	9.9
40	6.8	7.5	9.2	11.7	11.8	11.7
45	7.5	8.3	11.1	12.6	13.0	13.0
50	7.7	9.1	14.2	13.3	14.0	14.1
55	8.4	9.8	18.5	14.0	15.0	15.2
60	9.1	10.6	24.6	14.7	15.9	16.1
65				15.3	16.8	17.0
70				15.9	17.6	17.9
75				16.0	18.4	18.8
80				16.0	19.0	19.6

For MOF-303, the isotherm crossover phenomenon and crossover pressure confirms the presence of gas hydrates. Deviation between two isotherms after crossover pressure point did not expand rapidly possibly due to incomplete hydrate formation and uneven water distribution through the MOF-303 powder. One improvement for future studies could be to use MOF-water premix sample to ensure pores where hydrates formed. The key crossover is typically between 20 to 40 bars. MOF-303, also known for its exceptional water harvesting capabilities and stability [32], along with HKUST-1, exhibits high hydrophilicity but differs in water loading capacity, may influencing its behaviors towards hydrate formation. This underscores the necessity to synthesize and develop novel materials that can nucleate hydrates more rapidly at lower driving forces. Our findings also demonstrate that the presence of MOF makes hydrate crystallization less random and allows hydrate formation to be initiated without any mechanical energy within 6-8 hours. Further improvements in kinetics could be achieved by adding promoter-rich water, such as amino acids or surfactants.

HKUST-1 has internal pore diameter equal to 1.4 nm and 1.0 nm [33], causing faster diffusion of water molecule into HKUST-1. At higher Rw, HKUST-1 pores become super saturated with water. Even though pore sizes are not big enough to fit CH_4 hydrate crystals, it is possible that higher Rw in HKUST-1 leads to higher gas solubility in confined pore space. Thus at Rw = 2.36, gas adsorption contrition would come both from gas hydrate formed at outer surface as well as CH_4 gas over solubility in confined pore water.

 doi:10.20944/preprints202404.1006.v1

3.3.3. Effect of degree of wetness on gas adsorption

Figure.2 represents the high pressure isotherms by joining data from the key pressure points. The presence of water leads to lowering of the gas adsorption upto certain pressure. for example, in case of all nanoporous materials and for all Rw, total mmoles of CH_4 gas adsorbed decreased. Some of the material showed the crossover pressure pressure above which gas hydrate formation leads to total cumulative adsorption higher than the dry case. This crossover pressure depends on the surface chemistry (hydrophobic/hydrophilic), degree of wetness (Rw). As materials used in our research are known to have pore space lower than 1.2 nm (size of hydrate crystals), hydrates would only be formed at the outer surface of the MOFs surface.

Figure 2 presents the isotherm behavior for four different materials at various Rw values. Previous studies have shown that high-pressure isotherms demonstrate a drastic decrease in CH_4 adsorption in the hydrophilic material MIL-100 when water is present [15]. No hydrate formation was observed as Rw increased from 0 to 0.56. A crossover pressure was observed around 40 bar for R_w = 1.1. In the case of the hydrophobic ZIF-8, there was no significant reduction in CH_4 hydrate adsorption due to an increase in water. At higher Rw values of 0.2 and 0.6, crossover pressure was observed between 30 and 40 bar. The magnitude of this jump was dependent on the Rw value, with higher Rw leading to a larger increase.

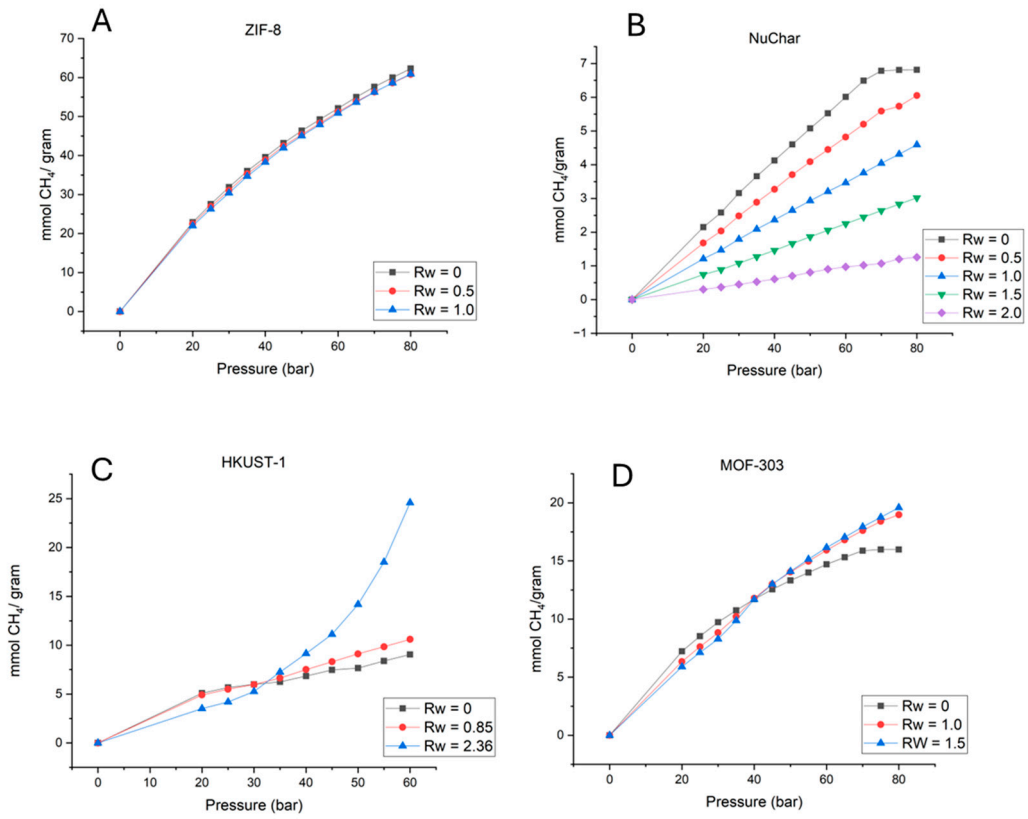

Figure 2. High pressure isotherms for dry and wet case Figure A, B represent the isotherms in ZIF-8 and Nuchar Carbon while Figure C, D represents high pressure isotherms in HKUST-1 and MOF 303.

In our studies, we found that an increase in the water amount in ZIF-8 did not lead to a drastic reduction in CH_4 adsorption values. However, for HKUST-1 and MOF-303, an increase in Rw led to a lower CH_4 adsorption value in wet conditions compared to dry conditions. For MOF-303, a crossover pressure was observed at P = 40 bar. Comparing data of MOF 303 and HKUST-1, crossover isotherms occurrences are not probabilistic in nature and indicate competitive adsorption phenomenon between H_2O and CH_4.

 doi:10.20944/preprints202404.1006.v1

3.3.4. Effect of Material Properties on Gas Adsorption

Two main properties that were a matter of research in this work were surface area and degree of hydrophilicity. Some of the key challenges associated with large volume would be uniform water distribution across the material. With large volume, we encounter mass transfer and heat transfer issues and further complexity of the equipment setup and crystals concentration would need further investigation.

Our studies indicate that hydrate formation is more likely to occur in hydrophilic materials than in hydrophobic materials with in large reactor when sample is used in large quantity. To compare the degree of hydrophilicity between MOF-303 and HKUST-1, we conducted water adsorption experiments. The results show that MOF-303 is slightly more hydrophilic compared to HKUST-1. Figure 3 shows the H2O isotherms at 298K showed the characteristics behavior of the MOFs with type 2 isotherm for HKUST-1 while type 4 isotherm for MOF-303. Thus water was filled in pores of MOF-303 at relatively lower pressure (≈ 0.2) as compared to HKUST-1. Above this relative pressure, isotherms show sharp increase in amount of water adsorbed. This increase is associated with the capillary condensation of H_2O molecules in the inner cavities of the MOFs (water condensation in mesocavities in inner space). H_2O sorption isotherms (298 K) were obtained using a vapor adsorption equipment known as VSTAR by Anton-Paar. Before the adsorption measurements, the samples were outgassed under vacuum at 423 K for 24 hours.

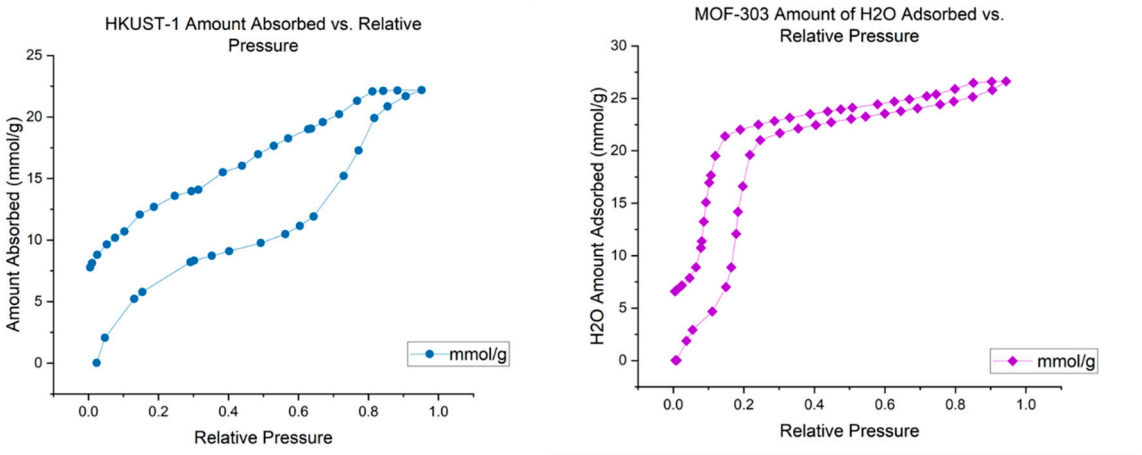

Figure 3. Water uptake (H_2O isotherms at 298K) of HKUST-1 and MOF-303.

3.4. Desorption Expriments

Desorption experiments were performed in few materials at selected Rw cases in continuation of the adsorption experiments. In previous studies, hydrate dissociation experiments were conducted on wetted porous materials in the presence of excess water [34]. Experiments with potential hydrate formation and/or higher Rw were selected for desorption experiments. It is evident through desorption experiments that, for a given Rw case of a MOF, the adsorbed CH4 amount corresponding to a pressure value is higher than that of the adsorption values for the same case. This seems plausible because it should be difficult for CH4 molecules to leave the MOFs after getting trapped inside their pores. Desorption studies indicate about the regeneration of the material for the next cycle.

 doi:10.20944/preprints202404.1006.v1

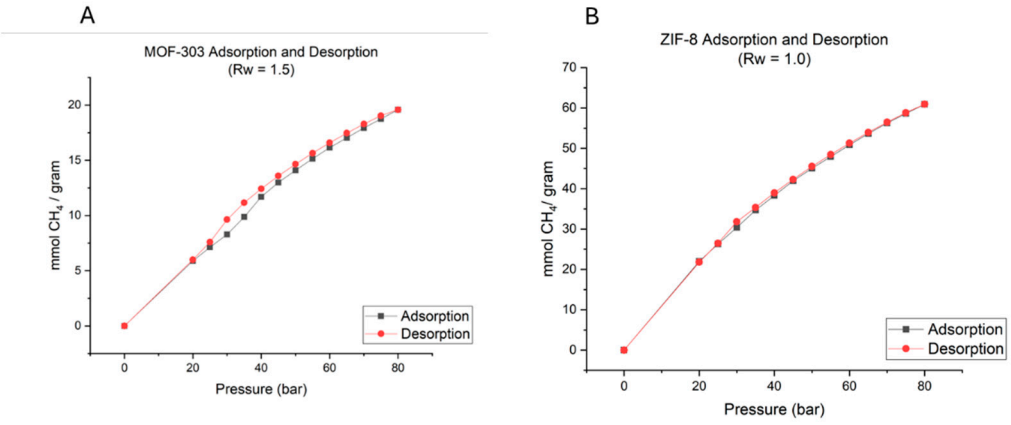

Figure 4. Adsorption and desorption experiment.

3.5 Material Stability

3.5.1. Material Visualization before and after Experiment

Below are the sample picture after different stages of the experiment to demonstrate the change in material color and texture. SEMs and XRD analysis do not suggest any major damage to crystals.

Figure 5. Change in sample color and texture before and after the experiments.

Colors and texture do not appear to change a lot however, MOFs in the presence of water tied to lump together.

3.5.2. SEM Images Visualization

SEM images (Refer to Figure 6) were acquired with a HITACHI S4800 field emission microscope operating at 2 kV in secondary electron and backscattered electron modes. Samples were prepared by drying a diluted dispersion of the particles in methanol on a silicon wafer substrate. SEM Images indicate the relatively larger size of HKUST-1 as compared to MOF 303 and ZIF 8 thus confirming the lower reported surface area (600 m^2/g) as compared to ZIF-8 and MOF 303 which had much

 doi:10.20944/preprints202404.1006.v1

smaller crystals. HKUST-1 crystals retained well faceted bipyramid octrahedral morphology after the testing under hydrate formation conditions.

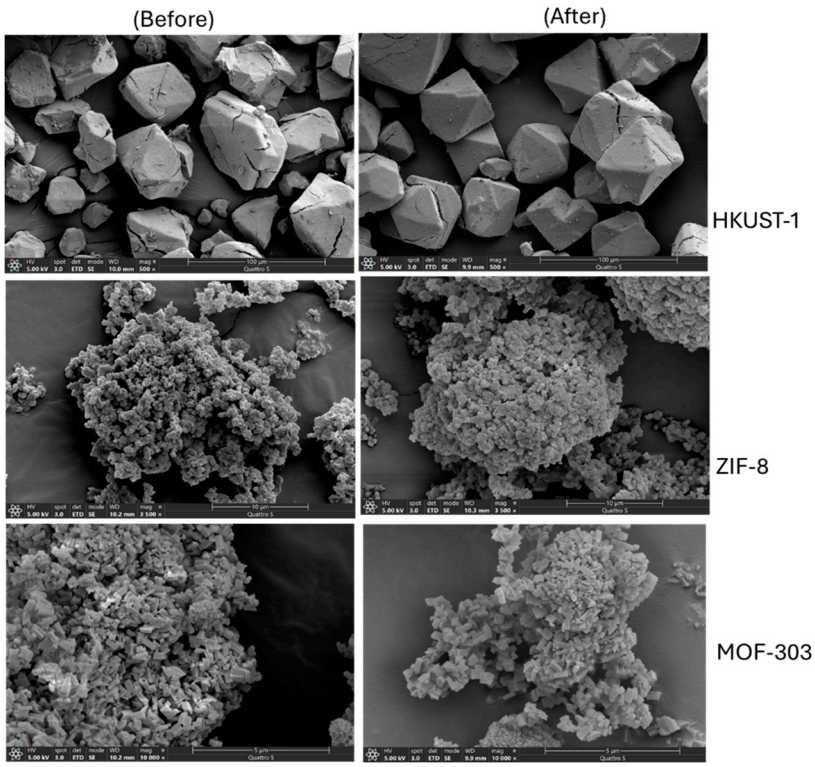

Figure 6. SEM Images before and after experiments (Dry case before experiment and final wet case after the experiment).

Figure 6 shows representative SEM images of the HKUST-1 sample before and after hydrate formation and dissociation studies. After hydrate formation, we did not see considerable increase in small particles on the surface of the HKUST-1 crystals confirming HKUST-1 stability in highly aqueous environment and under high pressure situations. This confirm HKUST-1 stability in highly aqueous environment but shorter exposure duration (around 6 days). For example, in other publication, HKUST-1 was exposed to water over a period of 28 days [35] and small particles were visible on the face of HKUST-1 crystals indicating the decomposition of material on account of water caused instability.

In case of ZIF-8, there are no remarkable changes in the morphology of the particles after series of the process including water saturation, adsorption, desorption in turn suggest that presence of water lead to agglomeration in the ZIF-8 particles which could also lead to smaller bed volume in aqueous environment [36]. No visible agglomeration was observed for HKUST-1. Studies show that HKUST-1 and ZIF-8 retains the crystallinity upto 100 MPa [37]. Thus hydrate formation pressure is expected to cause no harm on HKUST-1 or ZIF-8 crystalinity.

3.5.2. XRD Diffraction Pattern

X-ray diffraction analysis of the crystalline powder of samples was performed using a Bruker D8-Advance Diffractometer. X-ray radiation of Cu Kα was used and the measurement range was 3°-50° (2θ) with a step of 0.02°. Power X Ray diffraction (XRD) were collected to further investigate to confirm if there is any change in structural characteristics of the MOF crystals. XRD diffraction was collected for material of Interest HKUST-1 and MOF 303 as they shown to have gas hydrate formation. Before analysis, Samples were dried at 373.13 K until their mass became constant. Figure 7 shows the powder XRD pattens for the MOFs crystals before and after hydrate formation in the large volume reactor. These images show that the crystals retained its well faceted. Most of the MOFs

 doi:10.20944/preprints202404.1006.v1

used in this study are already commercially developed thus research should be focused on the scalability. No apprant change occurred in the XRD pattern between pre and post experimnent MOF 303 samples after minimum 3 cycles of adsorption and desorption experiments and more than 6 days in aqueous environment. HKUST-1 crystals show some deviation that is previously also recognised by other researchers [3]. Authors describe this deviation on account of change in the preferential plane exposure of the plane (222) over other crystallographic planes. Change in intensity ratio before hydrate and after hydrate could be due to the higher concentration of crystallites [38]. Studies focused on water effect on HKUST-1 crystalinity show change in ratio of 200/222 and 220/222 ratio due to denification of HKUST 1 structure in the presence of water [39,40].

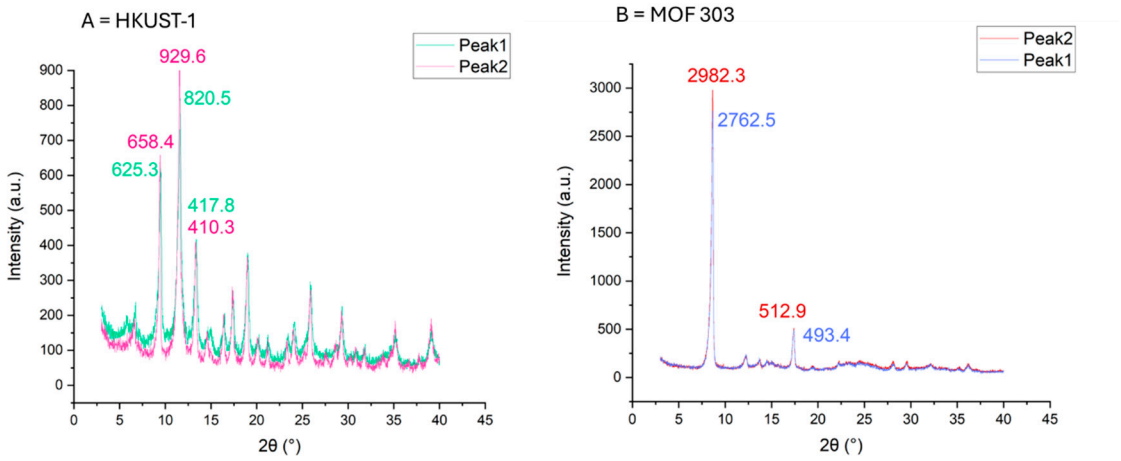

Figure 7. XRD data before (Peak 1) and after (Peak 2) the experiments.

We did not perform N_2 adsorption isotherm on residual/treated HKUST-1 sample after hydrate formation due to availability of data in other publications [3]. These studies show that pore volume decreased from 0.50 to 0.33 cm3/gram supporting the XRD observation and possible explanation behind densification of HKUST-1 on account of water and under high pressure. N_2 adsorption experiment for BET calculation confirms that HKUST-1 has lower surface area as compared to MOF-303. In case of ZIF-8, the organic linker 2-methylimidazole contribute to high hydrophobicity as indicated by water contact angle measurement.

4. Conclusions

In this research, for the first time, we explored the CH_4 adsorption in wet MOFs in a large-volume reactor. High-pressure isotherms were measured to investigate the beneficial role of gas hydrates in enhancing total gas adsorption. We identified a breakthrough pressure for hydrophilic materials, at which point isotherms with Rw>0 diverged from the isotherm with Rw=0 from below. This breakthrough pressure depends on the Rw amount as well as the surface chemistry. Both HKUST-1 and MOF-303 were shown to exhibit breakthrough pressure, stepped isotherms, and chemical stability after oversaturation and multiple adsorption cycles. Results also highlighted a discrepancy between large and small sample sizes for ZIF-8, as no hydrate formation was observed in repeated experiments in larger sizes. This discrepancy may be due to limitations in water/gas diffusion within powdered samples, an issue not encountered with very small sample sizes. The lab-based experimental methodology paves the way for future investigations under varied experimental conditions and temperatures. The findings of this study will further support the application of MOFs in large-scale reactors, enhancing scalability and the implementation of MOFs for large volumes.

Author Contributions: Conceptualization, methodology, investigation, project administration, supervision, writing- original draft preparation, and review and editing: Formal analysis, review & editing, funding acquisition: J.S.P; Investigation, Formal analysis. Original writing: N O; Supervision, project administration: N.v.S.

Funding: This research was funded by an international postdoctoral fellowship from the Independent Research Fund Grant Denmark (DFF), grant number 2031-00015B.

Conflicts of Interest: The authors declare no conflict of interest.

References

1. Koh, C.A. Towards a fundamental understanding of natural gas hydrates. *Chem. Soc. Rev.* **2002**, *31*, 157–167.
2. Pandey, J.S.; von Solms, N. Metal–Organic Frameworks and Gas Hydrate Synergy: A Pandora's Box of Unanswered Questions and Revelations. *Energies* **2023**, *16*.
3. Denning, S.; Majid, A.A.A.; Lucero, J.M.; Crawford, J.M.; Carreon, M.A.; Koh, C.A. Metal–Organic Framework HKUST-1 Promotes Methane Hydrate Formation for Improved Gas Storage Capacity. *ACS Appl. Mater. Interfaces* **2020**, *12*, 53510–53518.
4. Cuadrado-Collados, C.; Mouchaham, G.; Daemen, L.; Cheng, Y.; Ramirez-Cuesta, A.; Aggarwal, H.; Missyul, A.; Eddaoudi, M.; Belmabkhout, Y.; Silvestre-Albero, J. Quest for an Optimal Methane Hydrate Formation in the Pores of Hydrolytically Stable Metal–Organic Frameworks. *J. Am. Chem. Soc.* **2020**, *142*, 13391–13397.
5. Mazloomi, K.; Gomes, C. Hydrogen as an energy carrier: Prospects and challenges. *Renew. Sustain. Energy Rev.* **2012**, *16*, 3024–3033.
6. Wu, Z.; Wee, V.; Ma, X.; Zhao, D. Adsorbed Natural Gas Storage for Onboard Applications. *Adv. Sustain. Syst.* **2021**, *5*, 1–16.
7. Alhasan, S.; Carriveau, R.; Ting, D.S.K. A review of adsorbed natural gas storage technologies. *Int. J. Environ. Stud.* **2016**, *73*, 343–356.
8. Ma, S.; Zhou, H.-C. Gas storage in porous metal–organic frameworks for clean energy applications. *Chem. Commun.* **2010**, *46*, 44–53.
9. Kökçam-Demir, Ü.; Goldman, A.; Esrafili, L.; Gharib, M.; Morsali, A.; Weingart, O.; Janiak, C. Coordinatively unsaturated metal sites (open metal sites) in metal–organic frameworks: design and applications. *Chem. Soc. Rev.* **2020**, *49*, 2751–2798.
10. Kolle, J.M.; Fayaz, M.; Sayari, A. Understanding the Effect of Water on CO2Adsorption. *Chem. Rev.* **2021**, *121*, 7280–7345.
11. Denning, S.; Majid, A.A.A.A.; Lucero, J.M.; Crawford, J.M.; Carreon, M.A.; Koh, C.A. Methane Hydrate Growth Promoted by Microporous Zeolitic Imidazolate Frameworks ZIF-8 and ZIF-67 for Enhanced Methane Storage. *ACS Sustain. Chem. Eng.* **2021**, *9*, 9001–9010.
12. Farrando-Perez, J.; Balderas-Xicohtencatl, R.; Cheng, Y.; Daemen, L.; Cuadrado-Collados, C.; Martinez-Escandell, M.; Ramirez-Cuesta, A.J.; Silvestre-Albero, J. Rapid and efficient hydrogen clathrate hydrate formation in confined nanospace. *Nat. Commun.* **2022**, *13*, 5953.
13. Kim, D.; Ahn, Y.-H.; Lee, H. Phase Equilibria of CO 2 and CH 4 Hydrates in Intergranular Meso/Macro Pores of MIL-53 Metal Organic Framework. *J. Chem. Eng. Data* **2015**, *60*, 2178–2185.
14. Liu, H.; Zhan, S.; Guo, P.; Fan, S.; Zhang, S. Understanding the characteristic of methane hydrate equilibrium in materials and its potential application. *Chem. Eng. J.* **2018**, *349*, 775–781.
15. Casco, M.E.; Rey, F.; Jordá, J.L.; Rudić, S.; Fauth, F.; Martínez-Escandell, M.; Rodríguez-Reinoso, F.; Ramos-Fernández, E. V.; Silvestre-Albero, J. Paving the way for methane hydrate formation on metal-organic frameworks (MOFs). *Chem. Sci.* **2016**, *7*, 3658–3666.
16. Babaei, H.; DeCoster, M.E.; Jeong, M.; Hassan, Z.M.; Islamoglu, T.; Baumgart, H.; McGaughey, A.J.H.; Redel, E.; Farha, O.K.; Hopkins, P.E.; et al. Observation of reduced thermal conductivity in a metal-organic framework due to the presence of adsorbates. *Nat. Commun.* **2020**, *11*, 4010.
17. Cui, B.; Audu, C.O.; Liao, Y.; Nguyen, S.T.; Farha, O.K.; Hupp, J.T.; Grayson, M. Thermal Conductivity of ZIF-8 Thin-Film under Ambient Gas Pressure. *ACS Appl. Mater. Interfaces* **2017**, *9*, 28139–28143.
18. Lin, K.S.; Adhikari, A.K.; Ku, C.N.; Chiang, C.L.; Kuo, H. Synthesis and characterization of porous HKUST-1 metal organic frameworks for hydrogen storage. *Int. J. Hydrogen Energy* **2012**, *37*, 13865–13871.
19. Senkovska, I.; Kaskel, S. High pressure methane adsorption in the metal-organic frameworks Cu3(btc)2, Zn2(bdc)2dabco, and Cr3F(H2O)2O(bdc)3. *Microporous Mesoporous Mater.* **2008**, *112*, 108–115.
20. Peng, Y.; Krungleviciute, V.; Eryazici, I.; Hupp, J.T.; Farha, O.K.; Yildirim, T. Methane storage in metal-organic frameworks: Current records, surprise findings, and challenges. *J. Am. Chem. Soc.* **2013**, *135*, 11887–11894.
21. Prestipino, C.; Regli, L.; Vitillo, J.G.; Bonino, F.; Damin, A.; Lamberti, C.; Zecchina, A.; Solari, P.L.; Kongshaug, K.O.; Bordiga, S. Local structure of framework Cu(II) in HKUST-1 metallorganic framework: Spectroscopic characterization upon activation and interaction with adsorbates. *Chem. Mater.* **2006**, *18*, 1337–1346.
22. Mehio, N.; Dai, S.; Jiang, D. Quantum Mechanical Basis for Kinetic Diameters of Small Gaseous Molecules. *J. Phys. Chem. A* **2014**, *118*, 1150–1154.

 doi:10.20944/preprints202404.1006.v1

23. Chen, B.; Yang, Z.; Zhu, Y.; Xia, Y. Zeolitic imidazolate framework materials: recent progress in synthesis and applications. *J. Mater. Chem. A* **2014**, *2*, 16811–16831.
24. Banerjee, R.; Phan, A.; Wang, B.; Knobler, C.; Furukawa, H.; O'Keeffe, M.; Yaghi, O.M. High-Throughput Synthesis of Zeolitic Imidazolate Frameworks and Application to CO 2 Capture. *Science (80-.).* **2008**, *319*, 939–943.
25. Hwang, J.; Azzan, H.; Pini, R.; Petit, C. H 2 , N 2 , CO 2 , and CH 4 Unary Adsorption Isotherm Measurements at Low and High Pressures on Zeolitic Imidazolate Framework ZIF-8. *J. Chem. Eng. Data* **2022**, *67*, 1674–1686.
26. Fairen-Jimenez, D.; Moggach, S.A.; Wharmby, M.T.; Wright, P.A.; Parsons, S.; Düren, T. Opening the Gate: Framework Flexibility in ZIF-8 Explored by Experiments and Simulations. *J. Am. Chem. Soc.* **2011**, *133*, 8900–8902.
27. Moellmer, J.; Moeller, A.; Dreisbach, F.; Glaeser, R.; Staudt, R. High pressure adsorption of hydrogen, nitrogen, carbon dioxide and methane on the metal-organic framework HKUST-1. *Microporous Mesoporous Mater.* **2011**, *138*, 140–148.
28. Ortiz, G.; Nouali, H.; Marichal, C.; Chaplais, G.; Patarin, J. Energetic performances of the metal–organic framework ZIF-8 obtained using high pressure water intrusion–extrusion experiments. *Phys. Chem. Chem. Phys.* **2013**, *15*, 4888.
29. Khay, I.; Chaplais, G.; Nouali, H.; Marichal, C.; Patarin, J. Water intrusion–extrusion experiments in ZIF-8: impacts of the shape and particle size on the energetic performances. *RSC Adv.* **2015**, *5*, 31514–31518.
30. Küsgens, P.; Rose, M.; Senkovska, I.; Fröde, H.; Henschel, A.; Siegle, S.; Kaskel, S. Characterization of metal-organic frameworks by water adsorption. *Microporous Mesoporous Mater.* **2009**, *120*, 325–330.
31. Zhao, Z.; Wang, S.; Yang, Y.; Li, X.; Li, J.; Li, Z. Competitive adsorption and selectivity of benzene and water vapor on the microporous metal organic frameworks (HKUST-1). *Chem. Eng. J.* **2015**, *259*, 79–89.
32. Zheng, Z.; Nguyen, H.L.; Hanikel, N.; Li, K.K.-Y.; Zhou, Z.; Ma, T.; Yaghi, O.M. High-yield, green and scalable methods for producing MOF-303 for water harvesting from desert air. *Nat. Protoc.* **2023**, *18*, 136–156.
33. Guthrie, S.; Huelsenbeck, L.; Salahi, A.; Varhue, W.; Smith, N.; Yu, X.; Yoon, L.U.; Choi, J.J.; Swami, N.; Giri, G. Crystallization of high aspect ratio HKUST-1 thin films in nanoconfined channels for selective small molecule uptake. *Nanoscale Adv.* **2019**, *1*, 2946–2952.
34. Anderson, R.; Llamedo, M.; Tohidi, B.; Burgass, R.W. Experimental Measurement of Methane and Carbon Dioxide Clathrate Hydrate Equilibria in Mesoporous Silica. **2003**, 3507–3514.
35. Decoste, J.B.; Peterson, G.W.; Schindler, B.J.; Killops, K.L.; Browe, M.A.; Mahle, J.J. The effect of water adsorption on the structure of the carboxylate containing metal-organic frameworks Cu-BTC, Mg-MOF-74, and UiO-66. *J. Mater. Chem. A* **2013**, *1*, 11922–11932.
36. Mu, L.; Liu, B.; Liu, H.; Yang, Y.; Sun, C.; Chen, G. A novel method to improve the gas storage capacity of ZIF-8. *J. Mater. Chem.* **2012**, *22*, 12246.
37. Bazer-Bachi, D.; Assié, L.; Lecocq, V.; Harbuzaru, B.; Falk, V. Towards industrial use of metal-organic framework: Impact of shaping on the MOF properties. *Powder Technol.* **2014**, *255*, 52–59.
38. Domán, A.; Czakkel, O.; Porcar, L.; Madarász, J.; Geissler, E.; László, K. Role of water molecules in the decomposition of HKUST-1: Evidence from adsorption, thermoanalytical, X-ray and neutron scattering measurements. *Appl. Surf. Sci.* **2019**, *480*, 138–147.
39. Majano, G.; Martin, O.; Hammes, M.; Smeets, S.; Baerlocher, C.; Pérez-Ramírez, J. Solvent-mediated reconstruction of the metal-organic framework HKUST-1 (Cu3(BTC)2). *Adv. Funct. Mater.* **2014**, *24*, 3855–3865.
40. Sun, X.; Li, H.; Li, Y.Y.; Xu, F.; Xiao, J.; Xia, Q.; Li, Y.Y.; Li, Z. A novel mechanochemical method for reconstructing the moisture-degraded HKUST-1. *Chem. Commun.* **2015**, *51*, 10835–10838.